# Young's Modulus of Two-Dimensional Ice from the Electrostatic Compression of Mercury/Water/Mercury Tunnel Junctions

John D. Porter and Alexis S. Zinn-Warner*

*Department of Chemistry, University of California, Berkeley and Lawrence Berkeley Laboratory, Berkeley, California 94720-1460*

(Received 20 June 1994)

Solid-water films thinner than 0.8 nm were confined between the mercury surfaces of a squeezable tunnel junction at 265 ± 3 K. Uniaxial compression of the films was performed electrostatically by changing the junction bias. Mean compressive displacements were calculated from the nonlinear current response of the junction. Young's moduli of stable ice bilayers were estimated to be 134 MPa ± 18% (stat) ± 70% (sys), or about 1%–2% of the value of bulk ice $I_h$. Moduli of ice "double bilayers" decreased with increasing film thickness, from a maximum of ~20% of the bulk value.

PACS numbers: 68.60.Bs, 46.30.Rc, 62.20.Dc, 73.40.Rw

The properties of dimensionally confined matter can be different from the properties of bulk matter. However, when interfacial interactions dominate the system, information is hidden about the "intrinsic" physics of confinement. We have studied water confined between mercury surfaces, a system where the wall-water interaction is relatively weak [1], and have reported previously on the dynamic structures of molecularly thin films of liquid (l) $HNO_3$(aq) [2] and liquid water [3] at 293–295 K. Here, we describe mechanical properties of molecularly thin films of solid water confined between liquid-mercury surfaces at 265 K.

Metal(s)/molecular spacer(s)/mercury)(l) tunnel junctions have been studied previously [4–6] using Langmuir-Blodgett techniques to prepare the solid molecular spacer. Our experimental approach was similar to that of Moreland *et al.* [7], who prepared squeezable AG(s)/naphthalene(s)/Ag(s) tunnel junctions by first forming the junction in liquid naphthalene, then solidifying the molecular spacer. In the experiments reported here, quasistable Hg(l)/$H_2O$(l)/Hg(l) junctions [2,3] of well-defined Hg-Hg separation $s$ and junction area $A_J$ were formed at 275 K, and then the temperature was lowered to 265 K at ~3 mK/s.

The apparatus was similar to the one described previously [3]. Vertically opposed Hg hemispheres were electroplated onto the polished ends of glass-encased Pt electrodes (76 $\mu$m diam.) and immersed in pure water. A pyrex tube (2.5 cm × 1.37 cm O.D.) mounted on the bottom electrode held the water and a Hg "getter," and it formed the core of a small Plexiglass thermostat jacket. A computer-controlled Neslab RTE-5DD circulating thermostat bath was used to define the junction temperature. Coarse $x$-$y$-$z$ alignment of the junction was performed in liquid water by moving the bottom electrode mechanically, and fine $\delta z$ movement was achieved under open- or closed-loop conditions by moving the top electrode piezoelectrically. When the water was solid, extremely fine $\delta s$ perturbation was achieved electrostatically. The apparatus and low-level circuitry were mounted in an insulated mild steel box which was purged with dry nitrogen gas. Vibration isolation was standard [8].

The junction is formed where the surfaces of the mercury hemispheres interact through the intervening water. The geometry of the junction is assumed to be a plane-parallel cylinder, of face area $A_J = \pi r_J^2$ and mean separation $s \ll r_J$ between the faces. In the all-liquid state, this junction geometry is defined quite precisely by the interfacial Gibbs energies, dispersion interactions, liquid water structuring, and mechanical properties of the system [2,3,9,10]. Freezing of the water is assumed to affect the values of $s$ and $A_J$, but not the junction geometry. Typical values calculated from our data using methods described elsewhere [2,3] were $r_J \approx 50$ nm and $s \approx 0.5$–$0.8$ nm. We observed that the frozen systems were generally not in thermodynamic equilibrium, and $r_J$ varied slowly, with long relaxation times. This had to be taken into account when designing experiments and analyzing data.

The stationary tunnel junction current $I_J$ was assumed to be a power series of the stationary junction bias $V_J$ at low junction bias [11]: $I_J(V_J, s, A_J) = I_0 + \alpha V_J + \beta V_J^2 + \gamma V_J^3 + \cdots$ where the parameters $I_0$, $\alpha$, $\beta$, and $\gamma$,... scale linearly with $A_J$ and are more complicated functions of $s$. For physically symmetric junctions $I_0 = \beta = 0$ [11,12], and our results were consistent with this, within our uncertainties, so $I_J \approx \alpha V_J + \gamma V_J^3$ described our data. The ratio $\gamma/\alpha$ is a convenient function of materials constants and junction separation $s$; it is independent of junction area $A_J$, and it can be calculated from theory [11,12].

A time-dependent bias $V_J = V_{dc} + \sqrt{2} V_f \sin(2\pi f t)$ was applied to the top electrode. The mean junction bias $-0.1\ \text{V} \le V_{dc} \le 0.1\ \text{V}$ from a 12-bit DAC (LabMaster) was analog-summed near the junction with a sinusoidal voltage of rms magnitude $V_f = 2.44$ mV and frequency $f = 200.0$ Hz from a PAR 5301A lock-in amplifier. The resulting instantaneous junction current $I_J$ was measured by connecting the bottom electrode to a remote PAR 5381 current preamplifier and then to the lock-in amplifier and an HP 3478A voltmeter.

0031-9007/94/73(21)/2879(4)$06.00 © 1994 The American Physical Society 

We postulate that the solid-water spacer is an elastic medium [13] of Young's modulus $E$ that responds linearly to a uniform, uniaxial traction imposed on the plane-parallel faces of the junction. In the Hg(l)/$H_2O$(s)/Hg(l) system, the externally imposed traction is the electrostatic attraction [14] of the mercury surfaces across the solid-water spacer. Hence, changing the junction bias perturbs $s$ and $A_J$. In the linear-response limit of infinitesimal strain [13],

$$s \approx s_0\left(1 - \frac{\varepsilon_J \varepsilon_0 V_J^2}{2Es_0^2}\right) \tag{1}$$

describes the junction separation as a function of bias, where $\varepsilon_J$ is the relative permittivity of the medium in the junction and $s_0$ is the junction separation at equilibrium at zero bias. For thin liquid-water films at metal surfaces, it is believed that $\varepsilon_J$ is much less than the bulk value [15,16]. Here, we have used $\varepsilon_J = 6.5$ [2,3,16] for the solid-water film, and we estimate a maximum systematic uncertainty of $\pm 70\%$ for $\varepsilon_J$ based upon the results of molecular dynamics simulation [15,17] and the value of the infrared optical dielectric constant of ice $I_h$ [18]. We assume instabilities that would lead to "pinching" of the junction are absent and that the van der Waals repulsion between the mercury and the water is essentially a hard-wall interaction which results in no significant strain component normal to the interface.

We and others [2,3,12,14] find that $\ln(\alpha) \approx a - bs_0$ described the Simmons model of electron tunnelling at zero bias, including static image-potential corrections to the barrier [11], where $\alpha = (\partial I_J/\partial V_J)$ at $V_J = 0$. This expression fits experimental data for HG(l)/$H_2O$(l)/Hg(l) junctions, and parameters appropriate for pure structured liquid water in our apparatus are [3] $a \approx 1.62$ and $b \approx 1.77 \times 10^{10}$ m$^{-1}$. Changes in $A_J$ that occur on freezing the water affect $a$ but not $b$. Because $\alpha$ and $\gamma$ vary linearly with $A_J$ but exponentially with $s$, elastic changes in $s$ dominate the instantaneous "geometric" perturbations to $I_J$.

Expanding $I_J$ in a Taylor series out to second order, ignoring cross terms, and assuming $A_J \approx$ const over the short time interval of a measurement ($\sim$10 s) yields

$$I_J(V_J, s : A_J) \approx I_J(V_{dc}, s_0 : A_J) + \left(\frac{\partial I_J}{\partial V_J}\right)_{V_{dc},s_0}(V_J - V_{dc}) + \left(\frac{\partial I_J}{\partial s}\right)_{V_{dc},s_0}(s - s_0) + \frac{1}{2}\left(\frac{\partial^2 I_J}{\partial V_J^2}\right)_{V_{dc},s_0}(V_J - V_{dc})^2 + \frac{1}{2}\left(\frac{\partial^2 I_J}{\partial s^2}\right)_{V_{dc},s_0}(s - s_0)^2, \tag{2}$$

which can be analyzed to yield experimental observables in terms of junction parameters.

We measured the Fourier components of $I_J$ at frequencies 0 (i.e., dc), $f$, and $2f$. Substituting appropriately for the terms in Eq. (2) using the expressions given above, keeping terms up to $V_{dc}^3$ and $V_f^2$, and solving for the rms amplitudes of the currents yields

$$I_{dc} = I_J + \frac{\sqrt{2}V_f^2(\beta + 3\gamma V_{dc})}{2} + \frac{\alpha b \varepsilon_J \varepsilon_0\left(V_f^2 V_{dc} + V_{dc}^3\right)}{2Es_0} + \cdots, \tag{3}$$

$$I_f = V_f(\alpha + 2\beta V_{dc} + 3\gamma V_{dc}^2) + \frac{\alpha b \varepsilon_J \varepsilon_0 V_f V_{dc}}{Es_0} + \cdots, \tag{4}$$

$$I_{2f} = \frac{(\beta + 3\gamma)V_f^2 V_{dc}}{2} + \frac{\alpha b \varepsilon_J \varepsilon_0 V_f^2 V_{dc}}{2\sqrt{2}Es_0} + \cdots. \tag{5}$$

Experimental $I_{dc}(V_{dc})$, $I_f(V_{dc})$, and $I_{2f}(V_{dc})$ data were fitted to polynomials in $V_{dc}$ using least-squares regression, and the significance of the coefficients was determined statistically [19]. Within our uncertainty, Eq. (3) reduced to $I_{dc} \approx \alpha V_{dc}$ and Eq. (4) reduced to $I_f \approx \alpha V_f$ over the range of $V_{dc}$ studied. So we measured $I_{dc}$ and used piecewise least-squares regression to calculate $\alpha$. $I_{2f}$ was measured simultaneously using the lock-in amplifier.

Equation (5) can be rearranged to remove the effects of creep and slowly changing $A_J$:

$$\frac{I_{2f}}{\alpha V_f^2} \approx \left(\frac{3\gamma}{2\alpha} + \frac{b\varepsilon_J\varepsilon_0}{2\sqrt{2}Es_0}\right)V_{dc}, \tag{6}$$

where the qunatity on the left-hand side is calculated from observable parameters that are measured simultaneously, and we have omitted the term in $\beta \approx 0$.

Representative experimental results are shown in Fig. 1 for $\alpha$ calculated from Eq. (3) and for second-harmonic data plotted according to Eq. (6). The $\alpha$ data show the two features that were commonly observed during an experiment, namely shallow "bowing" of $\alpha[V_{dc}(t)]$ that could have positive or negative curvature, and rapid changes in $\alpha$ that could be positive or negative going. Knowing that the electric fields in the junctions were as high as $2 \times 10^8$ V/m, we looked for systematic changes in $\alpha$ that could be due to field-induced ordering or phase transitions in the water [17,20], but we found none within our present experimental resolution. The $\alpha$ data were more consistent with slow increase and/or decrease of

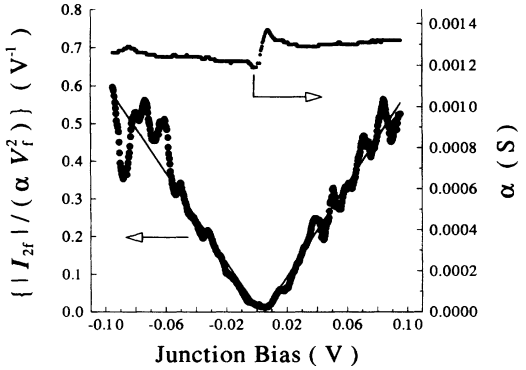


FIG. 1. Electrical characteristics of a Hg(l)/$H_2O$(s)/Hg(l) "ice-bilayer" junction, $s \approx 0.5$ nm, 265 ± 3 K. The dc current $I_{dc}$ and second harmonic current $I_{2f}$ were measured as the junction bias $V_{dc}$ was stepped incrementally from –0.1 to 0.1 V at a mean rate $\sim 10^{-4}$ V/s. The device conductance $\alpha$ was calculated from $I_{dc}(V_{dc})$ by numerical differentiation. The lines are least-squares fits to Eq. (6), and deviations lie within statistical bounds.

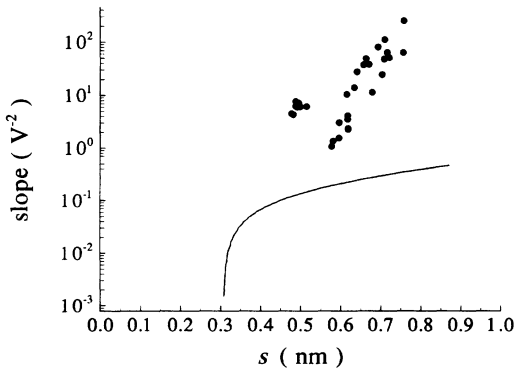


FIG. 2. Slope of second-harmonic plots like Fig. 1 as a function of tunnel junction thickness. Experimental data (points) are compared to the first term of Eq. (6) (line) calculated using the full Simmons model of electron tunnelling through a homogeneous dielectric medium. Model parameters were $\phi_{lim} = 2.92$ eV, $\varepsilon_J = 6.5$, $m^* = 0.96m_e$, and $r_J = 50$ nm.

$A_J$, possibly by plastic deformation and random stick-slip motion of the solid water at the junction perimeter. The stress driving this deformation seemed to be due mostly to the rapid solidification of the water in the apparatus and the "freezing in" of nonequilibrium junction geometries. Changes in $s$ cannot be ruled out from contributing to the changes in $\alpha$, but changes in $\alpha$ in Fig. 1 correspond to a change in $s$ of only 9 pm, or 2%.

We calibrated the second-harmonic response of our system using a half-wave rectifying signal diode in place of our junction, and we measured harmonic distortion of our instruments as a function of junction impedance by using a series of metal film resistors in place of the junction. Over the range of junction impedances studied here, background signals due to harmonic distortion varied from 0%–10% of typical nonlinear junction signals, and they were approximately independent of bias over our range of $V_{dc}$. Nontunnelling junctions behaved like linear circuit elements under our experimental conditions, with second-harmonic currents that did not differ from background. We also verified that $|I_{2f}|$ was a linear function of $V_f^2$ for the tunnelling junctions as given in Eqs. (5) and (6).

The second-harmonic data in Fig. 1 are fitted well by the model of Eq. (6), and variations in the data about the regression lines are within statistical uncertainties. There is good agreement between least-squares slopes at positive and negative bias. Similar behavior was observed for all junctions in which there was electron tunnelling, although the magnitude of the second harmonic signal varied with junction impedance.

Best-fit slopes from an analysis according to Eq. (6) are plotted as a function of junction impedance in Fig. 2, where the mean junction impedances $\alpha$ have been converted to approximate junction separations using the relationship given previously. We estimate maximum systematic uncertainties in $s$ due to variations in $A_J$ to be ±0.03 nm. There was a tight cluster of data at $s \approx$ 0.50 nm, then a spread of junction separations from 0.6 to 0.8 nm. This is similar to the pattern seen for liquid-water junctions [2,3], where a particularly stable separation was observed at $s = 0.50$ nm, no stable junctions were seen between $s = 0.5$ and 0.7 nm, and stable separations were observed around $s = 0.72$ nm and $s = 0.80$ nm.

The solid line in Fig. 2 is the first term of the slope of Eq. (6), calculated from the Simmons model [11], and it accounts for the inherent junction nonlinearity due to electron tunnelling through a finite potential barrier. The experimental data lie as much as 2 or more orders of magnitude above the line. Clearly, the second term in the slope of Eq. (6) dominates the experimental second harmonic response; i.e., the solid-water spacer in the junction is measurably compressible. The effect of junction compression is too small to have an impact in Eqs. (3) and (4), which contain dominant terms that are linear in $\alpha$.

Equation (6) was used to calculate Young's moduli for the solid-water spacers, using the Simmons model to calculate the ratio $\gamma/\alpha$. The results are shown in Fig. 3. For comparison, the mean value of $E$ for polycrystalline ice $I_h$ is about 9900 MPa [21]. The mean value of $E$ for the cluster of points at $s = 0.5$ nm, corresponding to the ice "bilayer," is 134 ± 24 (stat) MPa, which is about 1.4% of the value for bulk ice. Plugging this value back into Eq. (1), the compressional strain for the ice bilayer was 0.82% at a dc bias of 0.1 V, and the rms ac strain measured in response to the ac bias component was 5 ppm.

There was a discontinuity in $E(s)$ between $s = 0.5$ and 0.6 nm, which is consistent with a change in film structure. This shows that physical properties of molecular thin films can vary dramatically and nonmonotonically with small changes in film thickness. The modulus of the stable ice bilayer is significantly less than the maximum value observed for the multilayer. This is consistent with mechanical expectations based on the structural assignments made

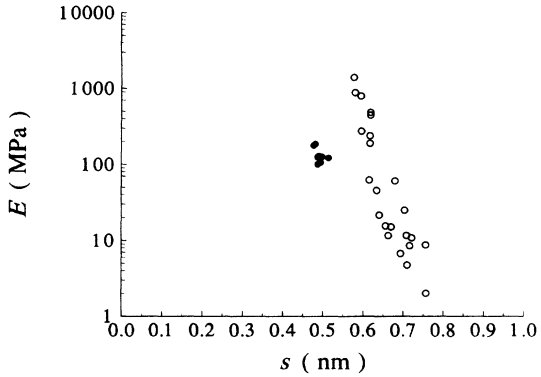


FIG. 3. Young's modulus for the solid-water films as a function of mean film thickness. The Simmons model was used to calculate junction separation $s$, assumed to be equal to mean film thickness, from the junction admittance at zero bias, $\alpha$. Experimental data were converted to Young's moduli using the model proposed here, Eq. (6). Data for water bilayers are shown as shaded points and those for water multilayers are shown as open points. The mean value for bulk ice $I_h$ is ~9900 MPa [21].

previously for liquid-water bilayers [3]. Assuming similar structures here, the bilayers show good H-bond connectivity in the plane but very small H-bond components normal to the plane. There are no H-bond "pillars" or closed cages normal to the surface in these bilayers [3], so the measured modulus reflects the relatively weak resistance of the H-bonded 2D lattice to soft distortion modes like torques and angular deformations. The intermolecular motions are too complex to interpret $E$ in terms of a potential surface, but extracting $E$ from an appropriate molecular dynamics simulation should be possible.

The ice "multilayer" data showed a wide variation of modulus with thickness, reaching a maximum value of about 2000 MPa of the thinnest multilayer, which is about 20% of the value for bulk ice $I_h$. The observation of higher limiting values of $E$ for the multilayers than for the bilayers would be consistent with the multilayers being "double bilayers" [2]. These multilayers are all postulated to contain a scaffold of closed H-bonded rings normal to the interface and a significant number of H bonds normal to the surface, i.e., H-bond pillars. In the liquid-water junction, multilayers have the shallowest Gibbs energy wells defining the equilibrium film thicknesses, permitting the system to sample a variety of junction separations with little energy penalty [2,3]. The results obtained here are consistent with quenching in of this structural freedom upon freezing of the liquid-water multilayers.

A infinite film thickness, the value of $E$ must equal the bulk value. The *decrease* observed in $E$ with increasing $s$ for the ice multilayers, all the way to our detection limit of $s \approx 0.8$ nm, shows that the approach to the bulk value is not monotonic with sample thickness. The observed decrease in $E$ for the thin films is consistent with increasing disorder in these films and concomitant weakening of the ordered scaffold of H-bond pillars as the films get thicker. This observation raises the intriguing possibility of confinement-driven order-disorder phase transitions occurring as a function of film thickness [22,23] in this system.

This work was supported by the Department of Energy through Grant No. DE-AC03-76SF00098 and the AT&T Foundation. We thank Mike Arndt and Tim Robinson for discussions.

*Present address: 3M Corporation, St. Paul, MN 55144.

[1] H. Sellers and P. V. Sudhakar, J. Chem. Phys. **97**, 6644 (1992).
[2] J. D. Porter and A. S. Zinn, J. Phys. Chem. **97**, 1190 (1993).
[3] J. D. Porter, Phys. Rev. Lett. (to be published).
[4] B. Mann and H. Kuhn, J. Appl. Phys. **42**, 4398 (1971).
[5] A. Sen and G. S. Singhal, J. Colloid Interface Sci. **68**, 471 (1979).
[6] A. F. Janzen and J. R. Bolton, J. Am. Chem. Soc. **101**, 6342 (1979).
[7] J. Moreland *et al.*, Appl. Phys. Lett. **43**, 387 (1983).
[8] C. J. Chen, *Introduction to Scanning Tunneling Microscopy* (Oxford University Press, New York, 1993), Chap. 10.
[9] K. L. Johnson, K. Kendall, and A. D. Roberts, Proc. R. Soc. London, Sect. A **324**, 301 (1971).
[10] J. N. Israelachvili, *Intermolecular and Surface Forces* (Academic Press, Orlando, Florida, 1985), Chap. 11.
[11] J. G. Simmons, J. Appl. Phys. **34**, 238; **34**, 1793 (1963). Typographical errors are corrected in Ref. [18].
[12] E. L. Wolf, *Principles of Electronic Tunneling Spectroscopy* (Oxford University Press, New York, 1985), pp. 36–46. The denominator of the 2nd term in Eq. (2.51) should be $32\bar{\phi}^{3/2}$.
[13] A. E. H. Love, *A Treatise on the Mathematical Theory of Elasticity* (Dover, New York, 1944), Chap. III.
[14] E. C. Teague, J. Res. Natl. Bur. Stand. Sect. A **91**, 171 (1986).
[15] J. Hautman, J. W. Halley, and Y-J. Rhee, J. Chem. Phys. **91**, 467 (1989).
[16] J. Goodisman, *Electrochemistry: Theoretical Foundations* (Wiley, New York, 1987), Chaps. 5 and 6.
[17] M. Watanabe, A. M. Brodsky, and W. P. Reinhardt, J. Phys. Chem. **95**, 4593 (1991).
[18] F. Franks, in *The Physics and Physical Chemistry of Water*, edited by F. Franks, Water: A Comprehensive Treatise Vol. 1 (Plenum Press, New York, 1972), Chap. 4.
[19] M. G. Natrella, in *Experimental Statistics,* NBS Handbook 91 (Wiley, New York, 1966), Chaps. 5 and 6.
[20] I. M. Svishchev and P. G. Kusalik, Phys. Rev. Lett. **73**, 975 (1994).
[21] *Gmelins Handbuch der Anorganischen Chemie, Sauerstoff 5* (Verlag Chemie, Weinheim, Germany, 1963), pp. 1444–1446.
[22] C. A. Murray and D. H. Van Winkle, Phys. Rev. Lett. **58**, 1200 (1987).
[23] C. A. Murray and R. A. Wenk, Phys. Rev. Lett. **62**, 1643 (1989).